ChemPubSoc Europe

DOI: 10.1002/chem.201902610

CHEMISTRY A European Journal Full Paper

Reactive Intermediates |*Hot Paper*|

Formation of Transient Anionic Metal Clusters in Palladium/Diene-Catalyzed Cross-Coupling Reactions

Marlene Kolter and Konrad Koszinowski*[a]

Abstract: Despite their considerable practical value, palladium/1,3-diene-catalyzed cross-coupling reactions between Grignard reagents RMgCl and alkyl halides AlkylX remain mechanistically poorly understood. Herein, we probe the intermediates formed in these reactions by a combination of electrospray-ionization mass spectrometry, UV/Vis spectroscopy, and NMR spectroscopy. According to our results and in line with previous hypotheses, the first step of the catalytic cycle brings about transmetalation to afford organopalladate anions. These organopalladate anions apparently undergo S_N2-type reactions with the AlkylX coupling partner. The resulting neutral complexes then release the cross-coupling products by reductive elimination. In gas-phase fragmentation experiments, the occurrence of reductive eliminations was observed for anionic analogues of the neutral complexes. Although the actual catalytic cycle is supposed to involve chiefly mononuclear palladium species, anionic palladium nanoclusters $[Pd_nR(DE)_n]^-$, ($n = 2$, 4, 6; DE = diene) were also observed. At short reaction times, the dinuclear complexes usually predominated, whereas at longer times the tetra- and hexanuclear clusters became relatively more abundant. In parallel, the formation of palladium black pointed to continued aggregation processes. Thus, the present study directly shows dynamic behavior of the palladium/diene catalyst system and degradation of the active catalyst with increasing reaction time.

Introduction

Palladium-catalyzed transformations, such as cross-coupling reactions, are among the most widely used tools in organic synthesis and, therefore, have been studied extensively. By now, the mechanisms of numerous reactions mediated by neutral, mononuclear palladium catalysts are thoroughly understood and have become classical textbook knowledge.[1,2] It is also generally recognized that palladium nanoparticles often exhibit high catalytic activities.[3–6] The size distribution of these nanoparticles can be reliably determined by microscopic methods. In contrast, far less is known about the intermediate size regime. The formation of nanoparticles from mononuclear precursors must proceed via so-called nanoclusters, which may also be released from nanoparticles in the reverse process. Thus, highly complex and dynamic mixtures of palladium species result, which have been aptly referred to as cocktail-type systems.[7,8] Several examples suggest that palladium aggregates display distinct reactivities. For instance, isolated dimeric palladium complexes, such as $[Pd_2X_2L_2]$ (X = Br, I; L = tBu$_3$P) have been found not only to be efficient precatalysts in Pd^0-mediated reactions,[9–12] but also to react directly with electrophilic substrates such as aryl iodides.[13–17] Similarly, isolated tri- and tetranuclear species have been demonstrated to mediate the dehydrogenation of formic acid[18–21] and C–C coupling reactions.[22,23] Clearly, such aggregates are of significant interest.

The difficulty in elucidating the behavior of palladium nanoclusters formed in situ lies in their transient nature and the scarcity of analytical methods capable of establishing their chemical identity. Under typical conditions, the aggregation of mononuclear palladium precursors is relatively fast and thus limits the lifetime of individual nanoclusters.[23–26] Moreover, the low-valent character of palladium nanoclusters presumably renders them susceptible to oxidation reactions. The transient nature of in-situ-formed nanoclusters excludes the use of crystallographic and microscopic methods for their characterization. Furthermore, the small size of nascent nanoclusters prohibits their analysis by dynamic light scattering. While viable, spectroscopic techniques, in turn, promise to afford only limited information on the molecular constitution of palladium nanoclusters.

Herein, we report the observation of transient anionic nanoclusters formed in palladium/diene-catalyzed cross-coupling reactions. As Kambe and co-workers have shown, this catalyst system works well for the coupling of alkyl halides with Grignard reagents.[27–31] The postulated reaction mechanism starts with the in situ formation of a mononuclear bis(η^3-allyl) palladium complex (Scheme 1).[27–31] The transfer of an organyl group from the Grignard reagent to the palladium center then affords an anionic intermediate, which undergoes oxidative ad-

[a] *M. Kolter, Prof. Dr. K. Koszinowski*
Institut für Organische und Biomolekulare Chemie
Universität Göttingen, Tammannstrasse 2, 37077 Göttingen (Germany)
E-mail: konrad.koszinowski@chemie.uni-goettingen.de

Supporting information and the ORCID identification number(s) for the author(s) of this article can be found under: https://doi.org/10.1002/chem.201902610.

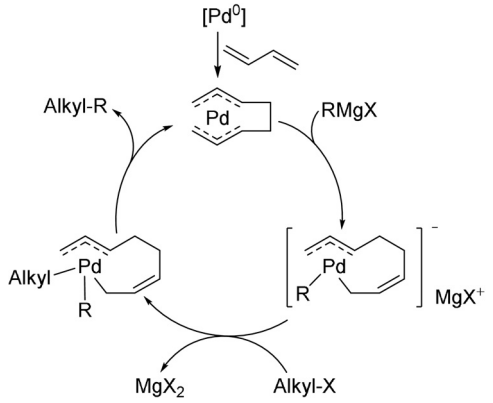

Scheme 1. Mechanism of palladium-catalyzed cross-coupling reactions between alkyl halides and Grignard reagents in the presence of buta-1,3-diene as suggested by Kambe and co-workers.[29,30]

dition of an alkyl halide in an S_N2-type process. The resulting heteroleptic neutral species releases the cross-coupling product in a reductive elimination and regenerates the bis(η^3-allyl) palladium complex.

Using electrospray-ionization (ESI) mass spectrometry as our chief analytical method, we provide the first experimental evidence of the invoked anionic palladate complexes in the title reactions. Besides the originally proposed mononuclear catalytic intermediate, we also found related palladium nanocluster anions in high signal intensities. ESI mass spectrometry offers the unique advantage of affording direct information on their aggregation states. The presence of the observed palladium nanoclusters and their further growth at longer reactions times point to a considerably higher complexity of the catalytic system than previously assumed. We complement our ESI mass spectrometric studies by gas-phase fragmentation experiments as well as UV/Vis and NMR spectroscopic measurements.

Results

Species formed by transmetalation

On analysis of a solution of the palladium(0) precatalyst $[Pd_2(dba)_3]$ (dba = dibenzylideneacetone), *n*BuMgCl, and isoprene (DE^I) in THF by negative-ion mode ESI mass spectrometry, the di- and tetranuclear organopalladate anions $[Pd_nBu(DE^I)_n]^-$ ($n = 2$ and 4) were detected as the main species (Figure 1; Figures S1 and S2, Supporting Information). Analogous low-valent nanoclusters were also observed when isoprene was replaced by buta-1,3-diene (DE^B; Figures S3–S5, Supporting Information) and when PhMgCl or BnMgCl was used as transmetalating agent (Figures S6–S20, Supporting Information). In contrast, trinuclear species ($[Pd_3Bu(DE^B)_4]^-$, $[Pd_3H(DE^B)_4]^-$, and $[Pd_3Bu(DE^B)_3]^-$; Figure S3 in the Supporting Information) proved to be less abundant and stable.

In all cases, the relative signal intensities of the palladate ions changed considerably over time (Figure 2 for the reaction of $[Pd_2(dba)_3]$ with PhMgCl and isoprene). When we probed sample solutions immediately after their preparation, we could

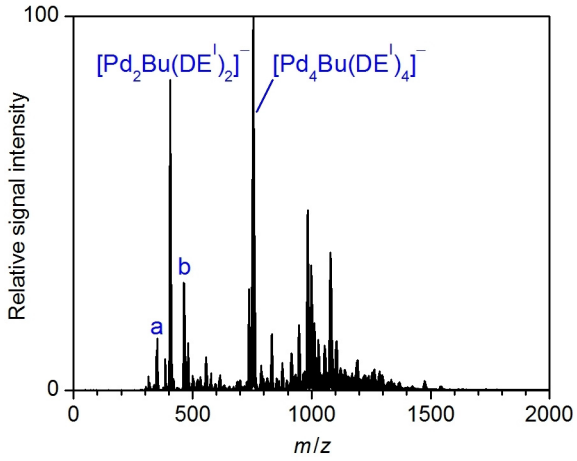

Figure 1. Negative-ion mode ESI mass spectrum of a solution of $[Pd_2(dba)_3]$ (1.5 mM), isoprene (DE^I, 24 mM), and *n*BuMgCl (12 mM) in THF (a = $[Pd_2H(DE^I)_2]^-$, b = $[Pd_2Bu_2H(DE^I)_2]^-$).

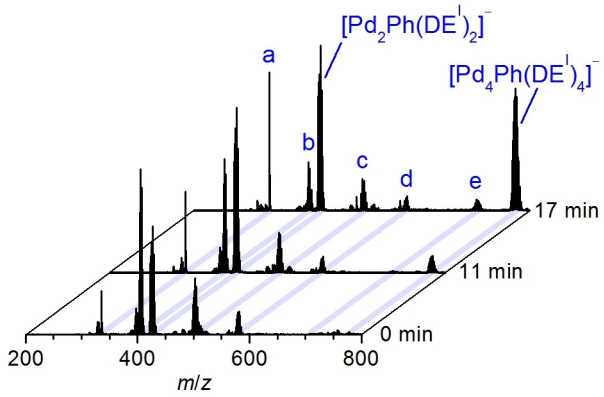

Figure 2. Negative-ion mode ESI mass spectra of a solution of $[Pd_2(dba)_3$ (1.5 mM), isoprene (DE^I, 24 mM), and PhMgCl (12 mM) in THF 0, 11, and 17 min after removal from the cooling bath 195 K, a = $[AlPh_4]^-$, b = $[PdPh_3(DE^I)]^-$, c = $[Pd_2Ph_2(DE^I)_2-H]^-$, d = $[Pd_2Ph_3(DE^I)_2]^-$, e = $[Pd_4Ph(DE^I)_3]^-$). $[AlPh_4]^-$ stems from aluminum impurities in the used Grignard reagent.

observe the low-valent mononuclear complexes $[PdR(DE^I)_2]^-$ (R = Bu, Ph) and $[PdPh(DE^I)]^-$ in low signal intensities (Figures S21–S26, Supporting Information). The mononuclear complexes were only short-lived and completely disappeared after a few minutes. In marked contrast, the relative signal intensity of the dinuclear and, in particular, of the tetranuclear nanoclusters increased with time. For solutions of $[Pd_2(dba)_3]$, BnMgCl, and isoprene, even the hexanuclear aggregate $[Pd_6Bn(DE^I)_6]^-$ could be detected after longer reaction times (Figures S19 and S20, Supporting Information). The absolute signal intensities of the observed palladate ions decreased with time. Besides palladates of the type $[Pd_nR(DE^I)_n]^-$, we also observed complexes $[Pd_nR_3(DE^I)_n]^-$ with palladium in higher average oxidation states (Figures S6, S10, S16, and S24, Supporting Information). In addition, hydride-containing species such as $[Pd_nH(DE^I)_n]^-$ and $[Pd_nR_xH_{3-x}(DE^I)_n]^-$ were also present in most cases (Figure 1 and Figures S3, S6, S10, S16, S19, and S21, Supporting Information).

To probe whether the palladate complexes preferentially incorporate isoprene or buta-1,3-diene, we performed competition experiments with the two compounds present in equimolar amounts (together with $[Pd_2(dba)_3]$ and *n*BuMgCl). In the resulting negative-ion mode ESI mass spectra, the signal intensities of the butadiene-containing palladates exceeded those of the complexes bearing both dienes, whereas hardly any palladates binding only isoprene were detected (Figures S27–S30, Supporting Information).

Control experiments with the palladium(II) precursors $PdCl_2$, PdI_2, and $Pd(OAc)_2$ combined with dienes and Grignard reagents did not yield any detectable organopalladate complexes. Instead, the resulting negative-ion mode ESI mass spectra were of only rather low absolute signal intensity and were dominated by nontransmetalated Pd^{II} complexes or heterobimetallic adducts such as $[Pd_2Cl_3(DE)]^-$ and $[MgPd_2Cl_5(DE)]^-$ (Figure S31, Supporting Information). Even with the Pd^0 precursor $[Pd_2(dba)_3]$, stable signal intensities could only be achieved when the precatalyst and the diene were allowed to react for at least 30 min before addition of the Grignard reagent.

In further control experiments, we replaced the Grignard reagent by organolithium and organozinc compounds. The transmetalation of $[Pd_2(dba)_3]$ with *n*BuLi in the presence of isoprene led to the formation of the palladate complexes $[Pd_nBu(DE^I)_n]^-$ ($n=2$, 4, 6) in high signal intensities. In addition, the mononuclear complexes $[PdBu(DE^I)]^-$ and $[PdBu(DE^I)_2]^-$ as well as several heterobimetallic complexes, such as $[LiPd_2Bu_2(DE^I)_4]^-$ and $[LiPd_3Bu_2(DE^I)_4]^-$, were observed (Figures S32–S34, Supporting Information). Like in the case of the reactions with the Grignard reagents, the mono- and dinuclear palladates rapidly disappeared, whereas the tetra- and hexanuclear ones increased over time (Figure S35, Supporting Information). After a few minutes, the overall signal intensity strongly decreased. No palladate complexes could be detected when *n*BuZnCl·LiCl was used as transmetalating agent (Figure S36, Supporting Information).

Analysis of the sample solutions by positive-ion mode ESI mass spectrometry showed abundant magnesium-containing cations, but no palladium complexes (Figure S37, Supporting Information). To obtain also insight into possibly formed neutral palladium species, we made use of a charge-tagged diene. In this way, quasineutral species incorporating this diene become amenable to ESI mass spectrometric analysis.[32,33] On treatment of a solution of $[Pd_2(dba)_3]$ and (*E*)-buta-1,3-dien-1-yltriphenylphosphonium bromide (DE^PBr^-) with *n*BuMgCl, we detected, among several palladium-free species, the complexes $[PdBu(DE^P)_2]^-$ and $[PdBuH(DE^P)(PPh_3)]$ (Figures S38–S47, Supporting Information; note that both of these species bear a total charge of +1 resulting from the positive charge of the DE^P units and the anionic or neutral character of the palladium center, as indicated in the given formulas). The former can be considered to be the cationized analogue of the mononuclear palladate anions discussed above. $[PdBuH(DE^P)(PPh_3)]$ corresponds to a true quasineutral species containing a free PPh_3 moiety, which presumably originated from decomposition of the charge-tagged diene. Among the observed palladium-free species, an ion with the sum formula of $C_{48}H_{49}P_2^+$ was of potential interest because its stoichiometry matches that expected for the addition product of two cationic diene molecules and a butyl anion.

UV/Vis spectroscopy showed that the band characteristic of $[Pd_2(dba)_3]$ (absorption maximum at $\lambda=520$ nm) did not change after the addition of isoprene (Figure S48, Supporting Information). Treatment with *n*BuMgCl led to a decrease of this band and to the appearance of a new absorption maximum at $\lambda=$ 450 nm along with a broad absorption at wavelengths between 500 and 700 nm (Figure 3). At longer reaction times, these absorption features decreased in intensity. Moreover, the precipitation of palladium black was observed by the naked eye.

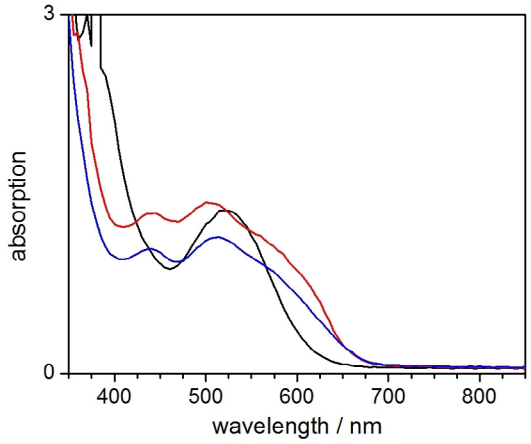

Figure 3. UV/Vis spectra of a solution of $[Pd_2(dba)_3]$ (1 mM) and isoprene (16 mM), stirred at 278 K for 50 min, before (black) and after the addition of 8 equiv of *n*BuMgCl after 1 min (red) and 120 min (blue) reaction time at 278 K.

To gain more information on the binding mode of the diene in the palladate complexes, we conducted NMR spectroscopic experiments. When isoprene was added to the palladium(0) precursor, the ^1H NMR signals of the former did not shift and were only slightly broadened (Figure S49, Supporting Information). On addition of PhMgBr to the solution, immediate broadening of the isoprene signals could be observed both in the ^1H and ^{13}C NMR spectra (Figure 4 and Figure S50, Supporting Information).

Unimolecular reactivity of organopalladates resulting from transmetalation

On fragmentation in the gas phase, the tetra- and hexanuclear $[Pd_nR(DE)_n]^-$ nanoclusters preferentially lost neutral $[Pd_2(DE)_2]$ (Eq. (1) with $n=4$ for DE^I and DE^B and 6 for DE^I; Figure 5; Figures S51–S57 and Table S1, Supporting Information). Further prominent fragmentation pathways resulted in the loss of single diene molecules (Eq. (2); Figures S51–S55 and S57–S62, Supporting Information).

$$[Pd_nR(DE)_n]^- \rightarrow [Pd_{n-2}R(DE)_{n-2}]^- + [Pd_2(DE)_2] \quad (1)$$

$$[Pd_nR(DE)_n]^- \rightarrow [Pd_nR(DE)_{n-1}]^- + DE \quad (2)$$

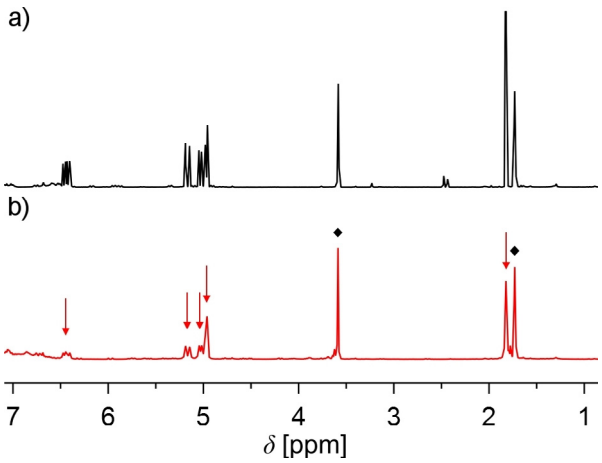

Figure 4. ^{1}H NMR spectra (400 MHz, [D$_8$]THF) of a mixture of [Pd$_2$(dba)$_3$] (25 mM) and isoprene (100 mM), a) before and b) after the addition of PhMgBr at 298 K. The signals marked with arrows correspond to isoprene, the signals at $\delta = 1.73$ and 3.58 ppm (◆) to THF.

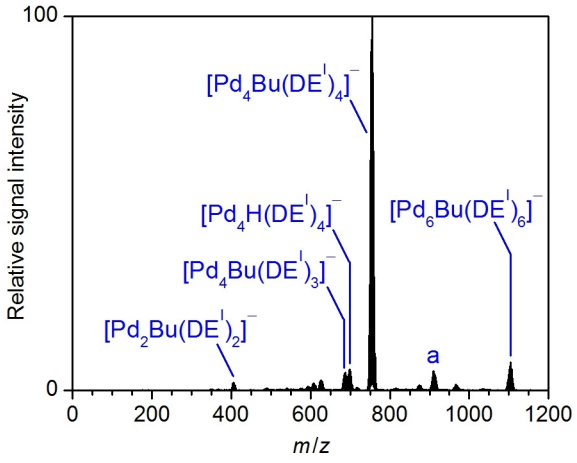

Figure 5. Mass spectrum of mass-selected [Pd$_6$Bu(DE^I)$_6$]$^-$ (DE^I = isoprene) and its fragment ions produced on collision-induced dissociation (E_{LAB} = 10.0 eV, a = [Pd$_6$H(DE^I)$_4$]$^-$).

Butyl-containing palladates also released butene (Eq. (3); Figures S51, S52, S55, S60, and S63–S65, Supporting Information).

$$[Pd_nBu(DE)_n]^- \rightarrow [Pd_nH(DE)_n]^- + C_4H_8 \quad (3)$$

All of these fragmentation processes occurred both as primary and consecutive reactions. In addition, we also observed product ions that showed the incorporation of dioxygen. Clearly, these species did not originate from fragmentation processes, but from ion–molecule reactions with residual traces of O_2 present in the vacuum system of the mass spectrometer.

For the cationized palladate [PdBu(DE^P)$_2$]$^-$, the main fragmentation pathway was the loss of butene (Figure S64, Supporting Information). In addition, it also afforded several other fragment ions stemming from ligand dissociation and ligand decomposition reactions. In contrast, the formation of the above-mentioned dimerization product $C_{48}H_{49}P_2^+$ was not observed. Other related DE^P-containing species, such as [PdBuH(DE^P)(PPh$_3$)], [PdBu(DE^P)$_2$(PPh$_3$)]$^-$, and [Pd(DE^P)(PPh$_3$)$_2$], also showed the elimination of butene and/or ligand dissociation and decomposition reactions (Figures S65–S67, Supporting Information).

Reactivity toward organyl halides

We next examined the reactivity of the in-situ-formed palladates toward propyl bromide as a prototypical substrate of cross-coupling reactions. When PrBr was added to a solution of [Pd$_2$(dba)$_3$], isoprene, and PhMgCl, [PdPh$_2$Pr(DE^I)$_n$]$^-$, n = 1 and 2, and the related hydride-containing complex [PdPh$_2$H(DE^I)$_2$]$^-$ were found (Figure 6). These intermediates apparently resulted from the reaction of [PdPh(DE^I)$_n$]$^-$ (n = 1 and 2) with PrBr. Interestingly, no analogous higher aggregates were observed. At longer reaction times, the propyl-containing palladates vanished and the [Pd$_n$Ph(DE^I)$_n$]$^-$ nanoclusters (n = 2, 4, and 6) reappeared (Figures S68 and S69, Supporting Information).

When BnMgCl was used as the transmetalating agent, the reaction with PrBr afforded [PdBn$_2$Pr(DE^I)$_2$]$^-$ and [PdBn$_2$H(DE^I)$_2$]$^-$, which were analogous to the intermediates formed from the phenyl-containing palladates (Figures S70–S76, Supporting Information). In contrast to the former case, the reaction of the benzyl-containing palladates now also yielded small quantities of the dinuclear complex [Pd$_2$Bn$_2$Pr(DE^I)$_2$]$^-$, which indicated reactivity of [Pd$_2$Bn(DE^I)$_2$]$^-$ toward PrBr. In addition, small amounts of [PdBn$_2$Pr(DE^I)]$^-$ and [PdBn$_2$H(DE^I)]$^-$ were observed. However, similar to the experiments without added PrBr, the obtained ESI mass spectra were dominated by [PdBn$_3$(DE^I)$_n$]$^-$ complexes (n = 0–3) .

On addition of PrBr to solutions of [Pd$_2$(dba)$_3$], isoprene, and *n*BuMgCl, the dinuclear complex [Pd$_2$Bu$_2$Pr(DE^I)$_2$]$^-$ formed, but exhibited only a short lifetime, comparable to that of [Pd$_2$Bu(DE^I)$_2$]$^-$ (Figures S77–S79, Supporting Information). In contrast, the tetranuclear cluster [Pd$_4$Bu(DE^I)$_4$]$^-$ reached its maximum signal intensity only after the decline of that of the

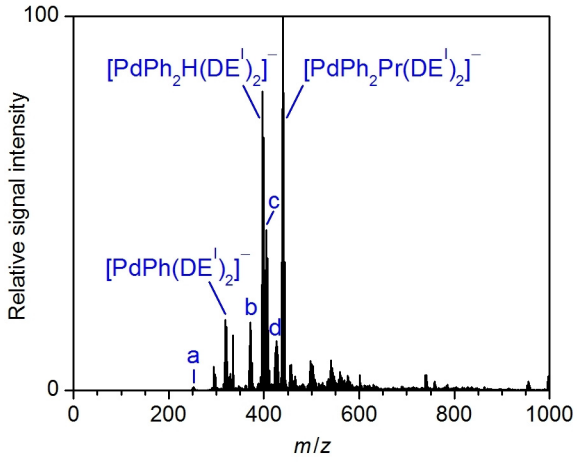

Figure 6. Negative-ion mode ESI mass spectrum of a solution of [Pd$_2$(dba)$_3$] (1.5 mM), isoprene (DE^I, 24 mM), PhMgCl (12 mM), and PrBr (12 mM) in THF (a = [PdPh(DE^I)]$^-$, b = [PdPh$_2$Pr(DE^I)]$^-$, c = [PdPh$_3$(DE^I)]$^-$, d = [Pd$_2$Ph(DE^I)$_2$]$^-$).

$[Pd_2Bu_2Pr(DE^I)_2]^-$ product complex (Figures S77–S79, Supporting Information). The reaction with PrI also furnished $[Pd_2Bu_2Pr(DE^I)_2]^-$ (Figure S80, Supporting Information), whereas that with PrCl or the secondary alkyl bromide *i*PrBr did not.

In a control experiment, we added the aryl iodide ethyl-4-iodobenzoate (ArI) to a solution of $[Pd_2(dba)_3]$, isoprene, and *n*BuMgCl. Aryl halides are not prone to undergo S_N2-type reactions and, therefore, should not readily react according to the mechanism postulated by Kambe and co-workers (Scheme 1). The control experiment did not show a palladate intermediate containing both a butyl and an aryl group, but instead resulted in the detection of $[PdArI_2]^-$ and $[PdArI_2(DE^I)]^-$, along with $[Pd_2I_3(DE^I)]^-$ and purely inorganic anions (Figure S81, Supporting Information). When the amount of ArI was reduced to 0.4 equiv (relative to *n*BuMgCl), $[PdArBuH(DE^I)_2]^-$ was observed as the main species (Figures S82–S89, Supporting Information). Other detectable species included $[PdArBuH(DE^I)]^-$, $[PdAr_2Bu(DE^I)]^-$, and $[PdArBu_2(DE^I)]^-$ along with $[Pd_2Bu(DE^I)_2]^-$, $[Pd_2Ar(DE^I)_2]^-$, $[PdAr(DE^I)_2]^-$, and $[PdAr(DE^I)]^-$.

To obtain additional information on possibly formed neutral intermediates, we also probed solutions of $[Pd_2(dba)_3]$, isoprene, *n*BuMgCl, and the charge-tagged substrate (6-bromohexyl)triphenylphosphonium bromide $(RBr)Br^-$. The resulting positive-ion mode ESI mass spectra showed [R−H], RBr, $(RBr)_2Br^-$, and very small amounts of the cross-coupling product RBu (Figure S90, Supporting Information). Increasing the quantity of the Grignard reagent to 3 equiv (relative to RBr) led to a higher signal intensity of the cross-coupling product (Figure S91). Negative-ion mode ESI showed $[PdBr_3R]^{2-}$ and, at higher concentrations of *n*BuMgCl, $[PdBrBuPhR]^{2-}$ and $[PdBu_2PhR]^{2-}$ as the only palladium-containing species (Figures S92–S95, Supporting Information). The last two ions apparently originated from decomposition of the triphenylphosphonium group of the charged tag.

Unimolecular reactivity of palladates resulting from the reactions with organyl halides

On gas-phase fragmentation, the palladate complexes formed from reactions with organyl halides preferentially underwent reductive eliminations (Figures S96–S100, Supporting Information). $[PdPh_2Pr(DE^I)_2]^-$ and, to a very small extent, $[PdPh_2Pr(DE^I)]^-$ reacted in this manner to give only the homo-coupling product (Eq. (4) with $n=1$ and 2; Figures S96 and S97, Supporting Information). In contrast, fragmentation of the dinuclear complex $[Pd_2Bu_2Pr(DE^I)_2]^-$ yielded both the cross- and the homo-coupling products in similar amounts (Figure S98, Supporting Information; Eqs. (5a) and (5b)), whereas that of $[PdAr_2Bu(DE^I)]^-$ gave the cross-coupling (Eq. (6)), but not the homo-coupling product (Figure S99, Supporting Information).

$$[PdPh_2Pr(DE^I)_n]^- \rightarrow [PdPr(DE^I)_n]^- + Ph_2 \quad (4)$$

$$[Pd_2Bu_2Pr(DE^I)_2]^- \rightarrow [Pd_2Bu(DE^I)_2]^- + PrBu \quad (5a)$$

$$\rightarrow [Pd_2Pr(DE^I)_2]^- + Bu_2 \quad (5b)$$

$$[PdBuAr_2(DE^I)]^- \rightarrow [PdAr(DE^I)]^- + ArBu \quad (6)$$

Further notable fragmentation reactions released hydrocarbons RH (Eq. (7) with R = Ph, Bn, and Bu; Figures S96–S98 and S101, Supporting Information).

$$[PdR_2Pr(DE^I)_n]^- \rightarrow [PdRPr(DE^I)_n{-}H]^- + RH \quad (7)$$

Discussion

Palladates in different aggregation states

The mononuclear complexes $[PdR(DE^I)_2]^-$ (R = Bu and Ph) found in the present study have exactly the same stoichiometry as the reactive intermediates that Kambe and co-workers have proposed to result from the transmetalation of a palladium(II) precursor.[29,30] Moreover, the corresponding cationized analogue became detectable when the charge-tagged diene was applied. The observation of this type of complex both in its anionic form and in its cationized form points to its facile formation under the given conditions.

However, our time-dependent measurements show that the mononuclear $[PdR(DE^I)_2]^-$ complexes have only rather short lifetimes and readily afford small nanoclusters $[Pd_nR(DE)_n]^-$ ($n=$ 2, 4, and 6). The predominance of nanoclusters with even numbers of palladium centers and their gas-phase fragmentation behavior imply that these species consist of dimeric subunits. A survey of low-valent palladium clusters reported in the literature reveals diverse structural motifs. Moiseev has shown that tetrameric palladium clusters can feature square, rectangular, or tetrahedral structures.[34] The geometry of these clusters is controlled both by the ligand environment and the formal oxidation state of the involved palladium centers. In addition, linear[35,36] and butterfly-shaped[21,37] structures are known.

Independent support for the formation of low-valent polynuclear palladium complexes in the sample solutions comes from the observation of a broad absorption band in the visible range. Such an absorption at higher wavelengths is commonly ascribed to the formation of palladium clusters.[24,25,38] Apparently, the palladium nanoclusters continue to grow beyond $[Pd_6R(DE)_6]^-$ and furnish even larger clusters, the *m/z* ratio of which lies outside of the probed range, and ultimately afford nanoparticles and metallic palladium. This assumption is fully in line with the observed precipitation of palladium black from the sample solutions.

Binding mode of the diene

The ESI mass spectrometric detection of palladate complexes containing just one diene unit and the loss of a single diene molecule on gas-phase fragmentation of the $[Pd_nR(DE^I)_n]^-$ ions are at odds with the dimerization of the diene and the formation of bis-allylic complexes postulated by Kambe and co-workers (Scheme 1). The signal broadening observed in the NMR spectra indicates a fast exchange between palladium-bound and free isoprene, but again does not give any evi-

dence of an allylic binding mode of the diene or its dimerization. We also considered the possibility that the observed ion with the sum formula of $C_{48}H_{49}P_2^+$ could have resulted from the coupling of a charge-tagged diene dimer and a butyl group brought about by a reductive elimination (Scheme S1, left, Supporting Information). However, the failure of the cationized palladate $[PdBu(DE^P)_2]^-$ to release $C_{48}H_{49}P_2^+$ on gas-phase fragmentation provides strong evidence against this hypothesis. Instead, $C_{48}H_{49}P_2^+$ presumably originated from the reaction of a butyl anion with one diene molecule followed by a consecutive addition to another diene unit (Scheme S1, right). Thus, our experiments do not give any indication for palladium-mediated diene dimerization under the present conditions. If such a dimerization takes place, it affects only a small fraction of the employed diene.

The competition experiments showed that the palladate complexes with buta-1,3-diene are more stable than those with isoprene. According to the results of Kambe and co-workers, the use of buta-1,3-diene affords significantly better yields in cross-coupling reactions than that of isoprene.[28] Apparently, the more stable diene palladate complexes are catalytically more active.

Decomposition processes

The formation of hydride-containing complexes can be easily rationalized for the use of *n*BuMgCl as transmetalating agent, because the palladium complexes resulting from the transfer of a butyl group can undergo β-hydride elimination (in the sample solution or during the ESI process). Our gas-phase fragmentation experiments directly showed the occurrence of these reactions. Indeed, the propensity of alkyl palladium complexes to undergo β-hydride eliminations is well known.[1] However, the observation of $[Pd_nPh_2H(DE)_m]^-$ (n, $m=1$, 2) and $[Pd_nBn_2H(DE)_m]^-$ (n, $m=1$–3) in the reactions with PhMgCl and BnMgCl, respectively, suggests the operation of alternative pathways that afford hydride-containing palladates. A possible mechanism furnishing these products consists of insertion of the diene into an organyl–metal bond followed by the elimination of a [(DE),R−H] diene, in which one hydrogen atom has been substituted by the organyl group R. Such a mechanism has recently been proposed to explain the presence of similar metal hydride complexes observed in cobalt/diene-catalyzed cross-coupling reactions.[39]

Another type of decomposition process appears to be involved in the formation of $[Pd_nR_xH_{3-x}(DE^I)_n]^-$ complexes, the average oxidation states of which are increased relative to $[Pd_nR(DE)_n]^-$. Possibly, they resulted from the latter by oxidation by residual traces of oxygen present in the sample solution and/or the mass spectrometer and consecutive transmetalation. The occurrence of such processes would indicate high susceptibility of the electron-rich palladate diene complexes to oxidation reactions. Alternatively, the complexes in higher oxidation states could also originate from the reaction of the low-valent palladates with remaining traces of RCl in the used Grignard reagents.[40]

Influence of palladium precursor and transmetalating agent

The inability of the palladium(II) precursors $PdCl_2$, PdI_2, and $Pd(OAc)_2$ to afford detectable organopalladate complexes on treatment with a diene and a Grignard reagent suggests that the diene molecules do not react with the nascent Pd^0 centers fast enough to prevent the occurrence of competing processes under the present conditions.[41] The need for relatively long incubation times of the $[Pd_2(dba)_3]$ precatalyst and the diene (before the addition of the Grignard reagent) also points to slow exchange reactions between the dba and diene ligands.

Among the different transmetalating reagents tested, *n*BuMgCl and *n*BuLi showed similar performance, whereas *n*BuZnCl·LiCl failed to produce detectable organopalladates. Presumably, this difference reflects the lower reactivity of organozinc reagents. Given that the latter are known to undergo highly efficient transmetalation reactions with Pd^{II} centers in Pd-catalyzed Negishi cross-coupling reactions,[42–45] the non-occurrence of analogous processes in the present case points to a diminished Lewis acidity of the palladium center. Such a diminished Lewis acidity is to be expected for palladium in an oxidation state of 0.

Catalytic cycle and role of palladium nanoclusters

The observation of a manifold of anionic palladate complexes in the present study suggests that anions are also involved in the catalytic cycle, as proposed by Kambe and co-workers. Although we were not able to confirm the postulated formation of neutral palladium bis-allyl species, we did detect the anions supposedly resulting from these species by transmetalation (Scheme 2). Our results strongly indicate that these anions contain not only dimerized, but also—and presumably predominantly—separate diene units (see above). As our experiments cannot directly distinguish between the actual catalytically active intermediates and the resting states of the catalyst, it could well be the case that complexes containing dimerized dienes correspond to the active species, but do not accumulate in significant concentrations due to their higher reactivity. The anionic intermediate then reacts with the alkyl halide in an S_N2-type process to afford a neutral complex, for which again the binding of both dimerized and separate diene units must be considered. Although we could not observe this neutral complex directly, we detected anionic analogues resulting from a further transmetalation reaction, that is, $[PdR_2Alkyl(DE)_n]^-$. In contrast, the $[PdArI_2(DE^I)_n]^-$ species found in control experiments with ArI substrates presumably originate from conventional oxidative additions, which correspond to the typical reactions between (neutral) Pd^0 complexes and aryl halides.

The decrease in signal intensity of the $[PdR_2Alkyl(DE)_n]^-$ intermediates at longer reaction times points to their consumption in consecutive reactions, as expected for a catalytic process. As our gas-phase fragmentation experiments directly demonstrate, these consecutive reactions correspond to reductive eliminations. The presence of two identical organyl groups R in the anionic complexes implies that the reductive elimina-

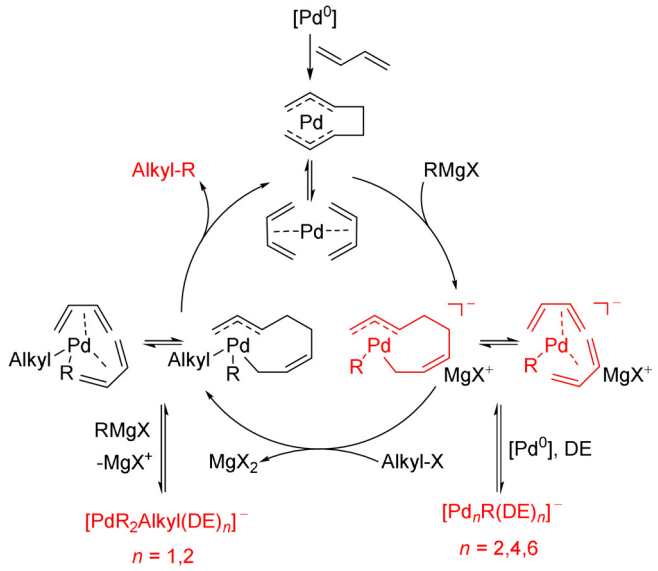

Scheme 2. Simplified catalytic cycle of a palladium-catalyzed cross-coupling reaction between an alkyl halide and a Grignard reagent in the presence of buta-1,3-diene. Species observed by ESI mass spectrometry (as shown or as isoprene-containing analogues) are highlighted. Note that the present experiments do not allow unambiguous differentiation between different isomers.

tion can furnish both the desired cross-coupling and the undesired homo-coupling product. Apparently, the branching between the cross- and homo-coupling channels is controlled by rather subtle effects and does not depend mainly on the electronic properties of the organyl substituents, as had been found for reductive eliminations from other transition-metal complexes.[46–49] This selectivity problem is avoided for reductive eliminations from the neutral complexes, which only bear a single R group. The high yields of the cross-coupling product obtained with palladium/diene catalysts in synthetic studies suggest that under typical conditions the reductive elimination occurs mainly at the stage of the neutral complexes. Indeed, neutral transition-metal complexes in general are known to undergo reductive eliminations more easily than the corresponding anionic ones.[46,48]

The full catalytic system is significantly more complex than the shown catalytic cycle based on mononuclear palladium complexes. In particular, the role of the observed anionic nanoclusters must be clarified. Apart from the dinuclear complexes $[Pd_2R_2Pr(DE^i)_2]^-$ (R = Bn and Bu), no aggregate incorporating an organyl substituent stemming from the organyl halide could be detected. This finding points to lower catalytic activities of the nanoclusters in comparison with the mononuclear complexes. For the palladium/diene-catalyzed reaction between *n*BuMgCl and PrBr, the time profiles of the different anions detected by ESI mass spectrometry exclude the direct participation of palladates $[Pd_nR(DE)_n]^-$ with $n>2$ in the catalytic process. Therefore, the main role of the palladium nanoclusters seems to be the provision of a reservoir for the reactive mononuclear complexes. The facile dissociation of the small clusters on gas-phase fragmentation suggests reversibility of the aggregation process. However, if cluster growth leads to the formation of larger nanoparticles and, eventually, palladium black, deterioration of the catalyst performance is to be expected. Thus, a highly dynamic nature of the catalytic system results.

Comparison with nickel/diene and cobalt/diene catalysts

As Kambe and co-workers have demonstrated, not only palladium/diene, but also nickel/diene[27] and cobalt/diene catalysts,[50] are effective in mediating alkyl–alkyl cross-coupling reactions between alkyl halides and Grignard reagents. Particularly the nickel-catalyzed reactions have been extensively investigated. In the course of these investigations, Kambe and co-workers isolated the anionic nickelate complex $[PhNi(\eta^1,\eta^3\text{-}C_8H_{12})]^-$ from a solution of $[Ni(cod)_2]$ (cod = cycloocta-1,5-diene), PhLi, buta-1,3-diene, and 12-crown-4 in high yields.[31] This complex contains two dimerized diene units and has a structure analogous to that of the palladate anion shown in Scheme 1. The apparently high tendency of nickel to mediate the dimerization of the diene contrasts the behavior of the palladates, which moreover showed only a lowered binding affinity to the diene. This lowered binding affinity gives rise to coordinately unsaturated complexes, which are prone to aggregation reactions and, ultimately, the formation of palladium black. In contrast, the mononuclear nickelate complexes are apparently much more stable. Presumably, this higher stability is one reason why cross-coupling reactions catalyzed by nickel/diene have been proven synthetically more useful than those catalyzed by palladium/diene.

Whereas no intermediate from cobalt/diene-catalyzed reactions has been isolated and structurally characterized, several cobaltate anions formed in situ have been identified by ESI mass spectrometry under conditions very similar to those of the present study, and thus allow direct comparison of the results. In the presence of a diene and a Grignard reagent, $CoCl_2$ mainly afforded $[CoH_xR_{2-x}(DE)_n]^-$ anions ($x=0$, 1; $n=2$–4).[39] These species differ from the palladate anions in several aspects:

1) The $[CoH_xR_{2-x}(DE)_n]^-$ complexes bear two organyl (or hydride) substituents, whereas the $[Pd_nR(DE)_n]^-$ complexes contain only one. This difference reflects the fact that cobalt has one valence electron less than palladium.
2) The cobaltate complexes incorporate a larger number of diene units than their palladate counterparts. This difference can be ascribed to a higher binding affinity of the diene to cobalt than to palladium and/or a higher tendency of the dienes to insert into Co–C than into Pd–C bonds.
3) In contrast to the palladates, the cobaltates do not form low-valent nanoclusters. The higher stability of the mononuclear cobaltates is in accordance with their supposedly higher binding affinity to the diene and their reluctance to form coordinatively unsaturated species, which then would aggregate.

Thus, although palladium, nickel, and cobalt all give organometallate anions on treatment with a Grignard reagent and a diene, the exact natures of these complexes differ considerably.

Conclusions

ESI mass spectrometry revealed the formation of anionic ate complexes in palladium/diene-catalyzed cross-coupling reactions. The transmetalation of $[Pd_2(dba)_3]$ with a Grignard reagent RMgCl or an organolithium compound RLi in the presence of a diene furnished $[Pd_nR(DE)_n]^-$ species ($n=1$, 2, 4, and 6). These complexes resemble a mononuclear palladate anion containing a dimerized diene moiety that Kambe and co-workers postulated in analogy to a known intermediate from nickel/diene-catalyzed reactions. However, the observed palladates show a lower tendency to bind dienes and to mediate their dimerization. The reduced diene affinity of the palladates and, accordingly, their lower average degree of coordinative saturation explain why they undergo aggregation reactions, which first afford nanoclusters and, eventually, palladium black. While the preponderance of even-numbered nanoclusters points to their formation from dinuclear subunits, the present results do not permit a more definite determination of their structures.

The observation of palladate anions bearing organyl substituents stemming from the RMgCl or RLi reagents shows that for the given catalytic cycle, as inferred by Kambe and coworkers, the transmetalation step precedes the oxidative addition of alkyl halides AlkylX. The latter apparently operates in an S_N2-type fashion and furnishes neutral intermediates, such as $[PdRAlkyl(DE^i)_n]$, which could not be detected in the present experiments. However, the formation of these species is suggested by the observation of related complexes $[PdR_2Alkyl(DE^i)_n]^-$, which are anionized by further transmetalation reactions. On gas-phase fragmentation, these anionic complexes predominantly undergo reductive eliminations. Besides the desired cross-coupling products RAlkyl, the reductive eliminations also yield homo-coupling products R_2. Such unwanted competing reactions are not to be expected for the actual catalytic cycle, because the putative neutral intermediates $[PdRAlkyl(DE^i)_n]$ cannot afford the homocoupling product.

The palladium nanoclusters have a lower tendency to react with organyl halides than their mononuclear congeners. Hence, they most likely do not correspond to the active catalytic intermediates themselves, but affect the catalytic cycle indirectly by tying up palladium atoms. The growth of the nanoclusters at the expense of the mononuclear complexes renders the whole catalytic system highly dynamic. Thus, the present case is another example of aggregation processes greatly increasing the complexity of palladium catalysis.

Experimental Section

General

To exclude moisture and oxygen, all experiments were carried out under standard Schlenk conditions. THF was dried with sodium/benzophenone and freshly distilled before use. PhMgBr in $[D_8]$THF and BnMgCl were synthesized according to literature procedures (see the Supporting Information). All other organometallic reagents were purchased. The concentrations of the organometallic reagents were determined by iodometric titration.[51] (*E*)-Buta-1,3-dien-1-yltriphenylphosphonium bromide and (6-bromohexyl)triphenylphosphonium bromide were synthesized in analogy to procedures reported in the literature.[52–54]

Sample solutions were prepared by dissolving $[Pd_2(dba)_3]$ in dry THF and addition of the diene followed by stirring at room temperature for 45 min. The solutions were then cooled to 195 K before the organometallic reagent and, in some of the experiments, the organyl halide was added. The resulting solutions were analyzed immediately.

ESI mass spectrometry

Sample solutions were transferred into the ESI source of a micrOTOF-Q II mass spectrometer (Bruker Daltonik) with gas-tight syringes at typical flow rates of 8 μL min^{-1}. In the experiment probing the reaction of $[Pd_2(dba)_3]$, isoprene, and *n*BuMgCl with PrI, the sample solution was kept in the cooled flask and transferred into the inlet line leading into the ESI source by applying a slight overpressure of Ar to enable detection of the short-lived complex $[Pd_2Bu_2Pr(DE^i)_2]^-$.[55,56] The ESI source was operated at a voltage of 3500 V with N_2 as nebulizer gas (flow rate of 5 L min^{-1}) and drying gas (0.7 bar backing pressure, temperature of 333 K). In simple MS^1 experiments, all generated ions with $50 \le m/z \le 3000$ were allowed to pass the quadrupole mass filter of the instrument. In MS^2 fragmentation experiments, ions of interest were mass-selected in the quadrupole mass filter, accelerated to a kinetic energy E_{LAB}, and allowed to collide with N_2 gas. Residual parent ions and resulting fragment ions were then detected after passage through the TOF analyzer. In most cases, accuracies of the measured *m/z* ratios of ≤ 25 ppm were obtained with an external calibration with a mixture of CF_3COOH and phosphazenes in H_2O/CH_3CN. In some cases, an internal calibration proved necessary. To this end, the *m/z* scale was adjusted to match the theoretical *m/z* ratio of an ion whose identity could be independently established with certainty (indicated for each experiment). Theoretical exact *m/z* ratios and isotope patterns were calculated with the DataAnalysis software package (Bruker Daltonik).

UV/Vis spectroscopy

Time-dependent UV/Vis spectroscopic experiments were carried out with a Cary60 instrument (Agilent Technologies). Sample solutions were prepared and analyzed under argon atmosphere at 278 K in dry THF by using an Excalibur immersion probe (Hellma Analytics). Spectra were recorded over a wavelength range of 350–1100 nm with a resolution of 5 nm.

NMR Spectroscopy

NMR spectra were recorded with a Bruker Avance III 400 instrument operating at 400 MHz (^{1}H) or 100 MHz (^{13}C) or a Bruker Avance III HD 300 instrument at 298 K. The chemical shifts were calibrated relative to the solvent signals ($[D_8]$THF: 1.73 ppm (^{1}H), 67.6 ppm (^{13}C)).

Acknowledgements

We thank Dr. Friedrich Kreyenschmidt for the synthesis of (*E*)-buta-1,3-dien-1-yltriphenylphosphonium bromide and (6-bromohexyl)triphenylphosphonium bromide and gratefully acknowledge funding from the CaSuS (Catalysis for Sustainable

Synthesis) program (scholarship for M.K.). Open access funding enabled and organized by ProjektDEAL.

Conflict of interest

The authors declare no conflict of interest.

Keywords: cluster compounds · cross-coupling · mass spectrometry · palladium · reactive intermediates

[1] C. Elschenbroich, *Organometallchemie*, Teubner, Stuttgart, **2003**.
[2] A. de Meijere, S. Bräse, M. Oestreich, *Metal-Catalyzed Cross-Coupling Reactions and More*, Wiley-VCH, Weinheim, **2014**.
[3] J. Durand, E. Teuma, M. Gómez, *Eur. J. Inorg. Chem.* **2008**, 3577 – 3586.
[4] A. Balanta, C. Godard, C. Claver, *Chem. Soc. Rev.* **2011**, *40*, 4973 – 4985.
[5] N. Yan, Y. Yuan, P. J. Dyson, *Dalton Trans.* **2013**, *42*, 13294 – 13304.
[6] C. Deraedt, D. Astruc, *Acc. Chem. Res.* **2014**, *47*, 494 – 503.
[7] V. P. Ananikov, I. P. Beletskaya, *Organometallics* **2012**, *31*, 1595 – 1604.
[8] D. B. Eremin, V. P. Ananikov, *Coord. Chem. Rev.* **2017**, *346*, 2 – 19.
[9] J. P. Stambuli, R. Kuwano, J. F. Hartwig, *Angew. Chem. Int. Ed.* **2002**, *41*, 4746 – 4748; *Angew. Chem.* **2002**, *114*, 4940 – 4942.
[10] T. J. Colacot, *Platinum Met. Rev.* **2009**, *53*, 183 – 188.
[11] M. Aufiero, F. Proutiere, F. Schoenebeck, *Angew. Chem. Int. Ed.* **2012**, *51*, 7226 – 7230; *Angew. Chem.* **2012**, *124*, 7338 – 7342.
[12] F. Proutiere, M. Aufiero, F. Schoenebeck, *J. Am. Chem. Soc.* **2012**, *134*, 606 – 612.
[13] K. J. Bonney, F. Proutiere, F. Schoenebeck, *Chem. Sci.* **2013**, *4*, 4434 – 4439.
[14] I. Kalvet, K. J. Bonney, F. Schoenebeck, *J. Org. Chem.* **2014**, *79*, 12041 – 12046.
[15] G. Yin, I. Kalvet, F. Schoenebeck, *Angew. Chem. Int. Ed.* **2015**, *54*, 6809 – 6813; *Angew. Chem.* **2015**, *127*, 6913 – 6917.
[16] M. Aufiero, T. Sperger, A. S.-K. Tsang, F. Schoenebeck, *Angew. Chem. Int. Ed.* **2015**, *54*, 10322 – 10326; *Angew. Chem.* **2015**, *127*, 10462 – 10466.
[17] M. Aufiero, T. Scattolin, F. Proutière, F. Schoenebeck, *Organometallics* **2015**, *34*, 5191 – 5195.
[18] I. Gauthron, J. Gagnon, T. Zhang, D. Rivard, D. Lucas, Y. Mugnier, P. D. Harvey, *Inorg. Chem.* **1998**, *37*, 1112 – 1115.
[19] D. Meilleur, D. Rivard, P. D. Harvey, I. Gauthron, D. Lucas, Y. Mugnier, *Inorg. Chem.* **2000**, *39*, 2909 – 2914.
[20] D. Meilleur, P. D. Harvey, *Can. J. Chem.* **2001**, *79*, 552 – 559.
[21] D. Evrard, D. Meilleur, M. Drouin, Y. Mugnier, P. D. Harvey, *Z. Anorg. Allg. Chem.* **2002**, *628*, 2286 – 2292.
[22] A. Sachse, M. John, F. Meyer, *Angew. Chem. Int. Ed.* **2010**, *49*, 1986 – 1989; *Angew. Chem.* **2010**, *122*, 2030 – 2033.
[23] A. Leyva-Pérez, J. Oliver-Meseguer, P. Rubio-Marqués, A. Corma, *Angew. Chem. Int. Ed.* **2013**, *52*, 11554 – 11559; *Angew. Chem.* **2013**, *125*, 11768 – 11773.
[24] J. Wang, H. F. M. Boelens, M. B. Thathagar, G. Rothenberg, *ChemPhysChem* **2004**, *5*, 93 – 98.
[25] A. V. Gaikwad, G. Rothenberg, *Phys. Chem. Chem. Phys.* **2006**, *8*, 3669 – 3675.
[26] D. A. Alonso, C. Nájera, *Chem. Soc. Rev.* **2010**, *39*, 2891 – 2902.
[27] J. Terao, H. Watanabe, A. Ikumi, H. Kuniyasu, N. Kambe, *J. Am. Chem. Soc.* **2002**, *124*, 4222 – 4223.
[28] J. Terao, Y. Naitoh, H. Kuniyasu, N. Kambe, *Chem. Lett.* **2003**, *32*, 890 – 891.
[29] J. Terao, N. Kambe, *Acc. Chem. Res.* **2008**, *41*, 1545 – 1554.
[30] N. Kambe, T. Iwasaki, J. Terao, *Chem. Soc. Rev.* **2011**, *40*, 4937 – 4947.
[31] a) T. Iwasaki, A. Fukuoka, X. Min, W. Yokoyama, H. Kuniyasu, N. Kambe, *Org. Lett.* **2016**, *18*, 4868 – 4871; b) T. Iwasaki, A. Fukuoka, W. Yokoyama, X. Min, I. Hisaki, T. Yang, M. Ehara, H. Kuniyasu, N. Kambe, *Chem. Sci.* **2018**, *9*, 2195 – 2211.
[32] K. L. Vikse, M. A. Henderson, A. G. Oliver, J. S. McIndoe, *Chem. Commun.* **2010**, *46*, 7412 – 7414.
[33] M. A. Schade, J. E. Fleckenstein, P. Knochel, K. Koszinowski, *J. Org. Chem.* **2010**, *75*, 6848 – 6857.
[34] I. I. Moiseev, *J. Organomet. Chem.* **1995**, *488*, 183 – 190.
[35] H. Kurosawa, *J. Organomet. Chem.* **2004**, *689*, 4511 – 4520.
[36] T. Murahashi, H. Kurosawa, *Coord. Chem. Rev.* **2002**, *231*, 207 – 228.
[37] K. Shimamoto, Y. Sunada, *Chem. Eur. J.* **2019**, *25*, 3761 – 3765.
[38] M. T. Reetz, M. Maase, *Adv. Mater.* **1999**, *11*, 773 – 777.
[39] F. Kreyenschmidt, K. Koszinowski, *Chem. Eur. J.* **2018**, *24*, 1168 – 1177.
[40] T. Gärtner, W. Henze, R. M. Gschwind, *J. Am. Chem. Soc.* **2007**, *129*, 11362 – 11363.
[41] Note that Kambe and co-workers have successfully used combinations of Pd^{II} precursors, 1,3-dienes, and Grignard reagents for cross-coupling reactions with alkyl (pseudo)halides, see ref. [28].
[42] J. A. Casares, P. Espinet, B. Fuentes, G. Salas, *J. Am. Chem. Soc.* **2007**, *129*, 3508 – 3509.
[43] B. Fuentes, M. García-Melchor, A. Lledós, F. Maseras, J. A. Casares, G. Ujaque, P. Espinet, *Chem. Eur. J.* **2010**, *16*, 8596 – 8599.
[44] M. García-Melchor, B. Fuentes, A. Lledós, J. A. Casares, G. Ujaque, P. Espinet, *J. Am. Chem. Soc.* **2011**, *133*, 13519 – 13526.
[45] J. Li, L. Jin, C. Liu, A. Lei, *Org. Chem. Front.* **2014**, *1*, 50 – 52.
[46] A. Putau, H. Brand, K. Koszinowski, *J. Am. Chem. Soc.* **2012**, *134*, 613 – 622.
[47] S. Weske, R. Schoop, K. Koszinowski, *Chem. Eur. J.* **2016**, *22*, 11310 – 11316.
[48] S. Weske, R. A. Hardin, T. Auth, R. A. J. O'Hair, K. Koszinowski, C. A. Ogle, *Chem. Commun.* **2018**, *54*, 5086 – 5089.
[49] T. Parchomyk, K. Koszinowski, *Chem. Eur. J.* **2018**, *24*, 16342 – 16347.
[50] T. Iwasaki, H. Takagawa, S. P. Singh, H. Kuniyasu, N. Kambe, *J. Am. Chem. Soc.* **2013**, *135*, 9604 – 9607.
[51] A. Krasovskiy, P. Knochel, *Synthesis* **2006**, 890 – 891.
[52] P. L. Fuchs, *Tetrahedron Lett.* **1974**, *15*, 4055 – 4058.
[53] D. E. Morrison, J. B. Aitken, M. D. de Jonge, F. Issa, H. H. Harris, L. M. Rendina, *Chem. Eur. J.* **2014**, *20*, 16602 – 16612.
[54] D. Rasina, M. Otikovs, J. Leitans, R. Recacha, O. V. Borysov, I. Kanepe-Lapsa, I. Domraceva, T. Pantelejevs, K. Tars, M. J. Blackman, K. Jaudzems, A. Jirgensons, *J. Med. Chem.* **2016**, *59*, 374 – 387.
[55] K. L. Vikse, M. P. Woods, J. S. McIndoe, *Organometallics* **2010**, *29*, 6615 – 6618.
[56] K. L. Vikse, Z. Ahmadi, J. Luo, N. van der Wal, K. Daze, N. Taylor, J. S. McIndoe, *Int. J. Mass Spectrom.* **2012**, *323 – 324*, 8 – 13.

Manuscript received: June 6, 2019
Revised manuscript received: July 11, 2019
Accepted manuscript online: July 23, 2019
Version of record online: September 17, 2019

